PERGAMON

International Journal of Heat and Mass Transfer 45 (2002) 291–301

International Journal of HEAT and MASS TRANSFER

www.elsevier.com/locate/ijhmt

Development of a diabatic two-phase flow pattern map for horizontal flow boiling

O. Zürcher *, D. Favrat [1], J.R. Thome [2]

Department of Mechanical Engineering, Swiss Federal Institute of Technology, CH-1015 Lausanne, Switzerland

Received 18 January 2001; received in revised form 17 April 2001

Abstract

An improved two-phase flow pattern map is proposed for evaporation in horizontal tubes. Based on new flow pattern data for three different refrigerants covering a wide range of mass velocities, vapor qualities and heat fluxes. The new flow pattern map includes the prediction of the onset of dryout at the top of the tube during evaporation inside horizontal tubes as a function of heat flux and flow parameters and is an extension to the flow pattern map model of Kattan et al. [J. Heat Transfer 120 (1998) 140]. The proposed modifications allow an accurate prediction of the flow pattern for very different fluids which are the substitute refrigerants (HFC-134a and HFC-407C) and the natural refrigerant R-717 (ammonia). © 2001 Published by Elsevier Science Ltd.

1. Introduction

The replacement of CFC refrigerants in refrigeration systems, heat pumps and organic Rankine cycles requires a good knowledge of the heat transfer and pressure drop properties of the substitute fluids. A contribution to this international effort is proposed with the study of two hydrofluorocarbon refrigerants (HFC-134a and the zeotropic mixture HFC-407C) and the study of the natural refrigerant ammonia.

Two-phase flow patterns are reported in tubular sight glasses located directly at the exit of 3.01 m long heat transfer test sections. The experimental test section is composed of two concentric tubes, with evaporation of the refrigerant inside the inner tube and counter-current water heating in the annulus. A new database of two-phase flow patterns for the refrigerants HFC-134a, HFC-407C and ammonia has been collected and used to develop a new and more general two-phase flow pattern map for horizontal tubes.

Within the range of the present tests, four of the six main flow patterns have been observed, i.e. stratified flow (S), stratified-wavy flow (SW), intermittent flow (I) and annular flow (A). The other two types of flow patterns (bubbly and mist flows) were not observed as they occur at flow rates higher than the operating limits of the test facility.

Kattan [2] made a review of flow pattern map models. Comparing those of Taitel and Dukler [3], Hashizume [4], Klimenko and Fyodorov [5] and Steiner [6] to his database of five refrigerants, he concluded that the most accurate was that of Steiner [6]. Kattan et al. [1] proposed a modified version of Steiner's map to take into account the effect of heat flux on the onset of dryout and to improve the stratified-wavy to annular transition prediction. Moreover they converted it into an easier format to use. Very good agreement has been found with the map of Kattan et al. [1] for HFC-134a, HFC-402A, HFC-404A, HFC123, CFC-502 and HFC-407C. Nevertheless, the prediction of the stratified to stratified-wavy transition still required perfection since the minimum mass velocities they tested did not reach that transition for the fluids considered.

Following the general concept of Kattan et al. [1] and based on the void fraction study and the assumptions of the model of Steiner [7], some new adaptations to his

* Corresponding author.

E-mail addresses: olivier.zuercher@epfl.ch (O. Zürcher), daniel.favrat@epfl.ch (D. Favrat), john.thome@epfl.ch (J.R. Thome).

[1] Director of the Laboratory for Industrial Energy Systems (LENI).

[2] Director of Laboratory for Heat and Mass Transfer (LTCM).

0017-9310/02/$ - see front matter © 2001 Published by Elsevier Science Ltd.
PII: S0017-9310(01)00146-6

Nomenclature

A	cross-sectional area (m^2)
B_r	pressure drop function (Pa)
D	diameter (m)
D_h	hydraulic diameter (m)
Fr	Froude number (dimensionless)
G	mass velocity [kg/(m^2 s)]
g	acceleration of gravity (m/s^2)
G_1, G_2	heat flux functions (dimensionless)
Δh_{evap}	latent enthalpy (J/kg)
h_L	liquid height in the tube (m)
$\dot{q}$	heat flux (W/m^2)
Re	Reynolds number (dimensionless)
S	contact perimeter (m)
s	sheltering coefficient (dimensionless)
T	temperature (K)
u	velocity (m/s)
We	Weber number (dimensionless)
x	vapor quality (dimensionless)
X_{tt}	Martinelli parameter (dimensionless)

Greek symbols

α	void fraction (dimensionless)
δ	liquid layer thickness (m)
θ_{wet}	wetted angle (rad)
λ	friction factor (dimensionless)
μ	dynamic viscosity (Pa s)
v	angle of evaporator ($=0$) (rad)
ξ_{Ph}	non-dimensional factor (dimensionless)
ρ	density (kg/m^3)
σ	surface tension (N/m)

Subscripts

A	annular
crit	critical
I	intermittent
i	interface
L	liquid
MF	mist flow
Strat	stratified
Wavy	stratified-wavy
V	vapor
wet	wetted
(˜)	non-dimensional value of a parameter

original flow map are proposed here to obtain a new flow pattern map that better agrees with fluids of quite different physical properties like ammonia. Rather than first showing the flow pattern data and then the proposed modifications to the transition equations, the observations will be presented afterwards to avoid their repetition.

2. Generalities on flow pattern

2.1. The stratified flow pattern

The stratified flow pattern is characterized by the separation of the liquid and vapor phases by a smooth interface. This flow pattern occurs at very low mass velocities when the Kelvin–Helmholtz instability criterion is counter-balanced by the viscous forces. Fig. 1 depicts the cross-section of stratified two-phase flow. The areas designated by A are cross-sectional areas and S refers to the characteristic lengths (perimeter and interface). The internal diameter is D. The subscripts refer to vapor (V), liquid (L) and the interface (i). The geometrical relationships for this flow pattern are as follows:

$$S_L = D\frac{\theta_{wet}}{2}, \tag{1}$$

$$S_V = D\left(\pi - \frac{\theta_{wet}}{2}\right), \tag{2}$$

$$S_i = D\sin\left(\frac{\theta_{wet}}{2}\right), \tag{3}$$

$$A_L = \frac{D^2}{8}[\theta_{wet} - \sin\theta_{wet}], \tag{4}$$

$$A_V = \frac{D^2}{8}[2\pi - 2\theta_{wet} + \sin\theta_{wet}] = A - A_L. \tag{5}$$

Finally the liquid height is:

$$h_L = \frac{D}{2}\left(1 - \cos\frac{\theta_{wet}}{2}\right). \tag{6}$$

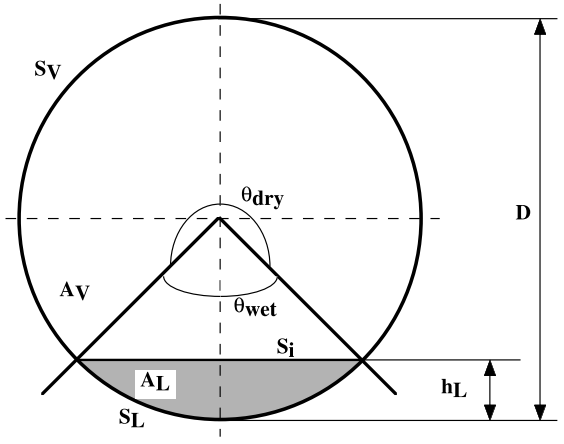

Fig. 1. Two-phase flow cross-section.

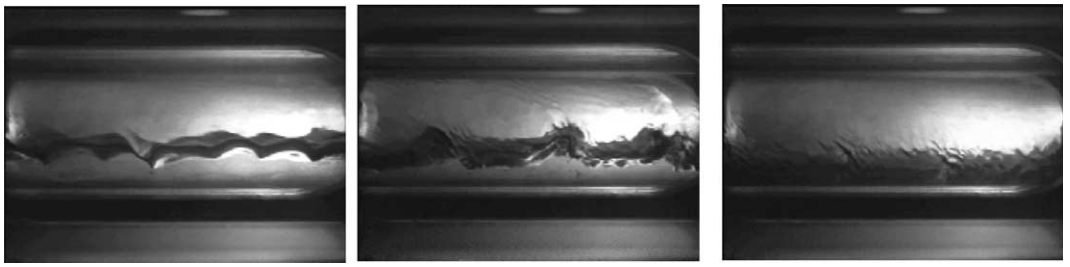

Fig. 2. Three different stratified-wavy flow patterns of pure ammonia flowing at $x = 0.20$ and $G = 26$ kg/m^2 s, $x = 0.20$ and $G = 60$ kg/m^2 s and $x = 0.80$ and $G = 41$ kg/m^2 s.

With respect to the stratified geometry, the liquid height is a direct function of void fraction.

2.2. The stratified-wavy flow pattern

The stratified-wavy flow pattern is characterized by a wavy interface of the liquid as shown in Fig. 2. This flow pattern is a transitional one where waves exist but these are of a reduced magnitude and are not able to reach the top of the tube. In a cross-sectional view, the interface is curved.

2.3. The annular flow pattern

The annular flow pattern is obtained when the liquid wets all the tube periphery with the vapor flowing at the center of the tube. Due to gravity, the film thickness is not uniform around the periphery but is thicker at the bottom. Fig. 3 depicts a video image of annular flow for ammonia.

The annular flow pattern has been considered to be reached when the motion of the liquid flowing at the top of the tube is comparable to that of the liquid at the bottom of the tube. Globally, the heat transfer coefficient for annular flows shows a constant increase in value with increasing vapor quality, until the breakup of the liquid film at the top of the tube occurs at the onset of dryout. The heat transfer coefficient reaches its peak at this point and then decreases very rapidly towards the value of the all vapor heat transfer coefficient. Thus, the onset of dryout in the annular flow regime is important for modelling heat transfer.

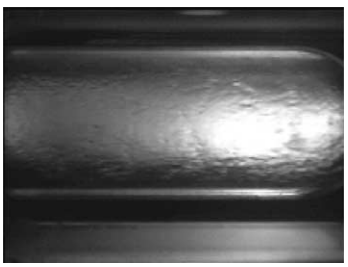

Fig. 3. Annular flow pattern of pure ammonia flowing at $x = 0.81$ and $G = 122$ kg/m^2 s.

2.4. The intermittent flow pattern

The intermittent flow pattern occurs at low vapor quality. It groups unsteady flow patterns like plug and slug flows. Due to the unsteadiness of the flow, the tube periphery is almost constantly wetted by the large amplitude waves that frequently wash the top of the tube. Fig. 4 shows two video images of intermittent flow for ammonia. The transition criterion between intermittent and annular flow is recognized to be mainly a function of void fraction. Between successive large amplitude waves, the flow pattern is temporarily stratified or stratified-wavy with a thin liquid film left behind around the top perimeter of the tube by the passing waves.

3. Description of the Kattan et al. flow pattern map

3.1. Equation of the S–SW transition

The model used to define the stratified to stratified-wavy transition is similar to the one developed earlier by Taitel and Dukler [3]. The transition is obtained when the pressure and the shear work on a wave overcome the viscous dissipation of the wave. Note that the description of the complete phenomenon has been admitted by both authors not to be complete but is still generally accepted. Steiner [7], however proposed using a smaller value of the sheltering coefficient $s = 0.005$ to finally obtain:

$$G_{\mathrm{Strat,Steiner}} = \left[226.3^2 \cdot \frac{\tilde{A}_{\mathrm{L}}\tilde{A}_{\mathrm{V}}^2 \rho_{\mathrm{V}}(\rho_{\mathrm{L}} - \rho_{\mathrm{V}})\mu_{\mathrm{L}} g \cos v}{\pi^3 x^2 (1-x)}\right]^{1/3}, \tag{7}$$

where $\tilde{A}_{\mathrm{L}} = A_{\mathrm{L}}/D^2$ and $\tilde{A}_{\mathrm{V}} = A_{\mathrm{V}}/D^2$ are non-dimensional cross-sectional areas. Thus, they are functions of void fraction. Kattan et al. [1] also adopted Eq. (7).

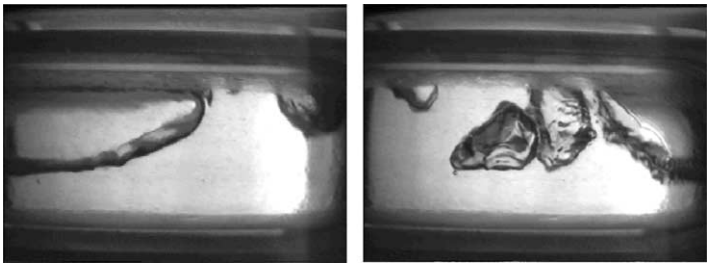

Fig. 4. Intermittent flow pattern of pure ammonia flowing at $x = 0.06$ and $G = 180$ kg/m^2 s. Both images are from the same video sequence.

Note that for horizontal flow, the angle v is equal to zero.

3.2. Equation of the SW–AI transition

Compared to the approach of Taitel and Dukler [3] and Steiner [7] included the effect of surface tension as a consequence of capillary waves to obtain:

$$G_{\text{Wavy,Steiner}} = \sqrt{\frac{16\tilde{A}_{\text{V}}^3 gD\rho_{\text{L}}\rho_{\text{V}}}{\pi^2 x^2\sqrt{1-(2\tilde{h}_{\text{L}}-1)^2}}\left[\frac{\pi^2}{25\tilde{h}_{\text{L}}^2}\left(\frac{Fr}{We}\right)_{\text{L}}+\frac{1}{\cos v}\right]}, \tag{8}$$

where cross-sectional areas and liquid height are presented in dimensionless form as originally proposed by Taitel and Dukler [3]: $\tilde{h}_{\text{L}} = h_{\text{L}}/D$, $\tilde{A}_{\text{V}} = A_{\text{V}}/D^2$, etc., and where:

$$\left(Fr\cdot\frac{1}{We}\right)_{\text{L}} = \left(\frac{u_{\text{L}}^2}{gD}\frac{\sigma}{\rho_{\text{L}}u_{\text{L}}^2 D}\right) = \frac{\sigma}{gD^2\rho_{\text{L}}}. \tag{9}$$

The Weber number We is the ratio of inertia to surface tension forces. The Froude number Fr is a ratio of inertia to gravity forces. Both are expressed with the diameter of the tube as characteristic length.

Kattan et al. [1] proposed two changes to the above boundary. First, they introduced the heat flux effect on the onset of dryout by modifying the Fr/We ratio in the following way:

$$(1-x)^{G_1}\left[\left(\frac{Fr}{We}\right)_{\text{L}}\right]^{G_2}, \tag{10}$$

where

$$G_1 = -48.24\left(\frac{\dot{q}}{\dot{q}_{\text{crit}}}\right) \tag{11}$$

and

$$G_2 = 9.65\left(\frac{\dot{q}}{\dot{q}_{\text{crit}}}\right)+1.053, \tag{12}$$

where $\dot{q}$ is the heat flux and $\dot{q}_{\text{crit}}$ is the critical heat flux for nucleate pool boiling calculated from the Kutateladze correlation, which is:

$$\dot{q}_{\text{crit}} = 0.131\sqrt{\rho_{\text{V}}}\Delta h_{\text{evap}}[g(\rho_{\text{L}}-\rho_{\text{V}})\sigma]^{1/4}. \tag{13}$$

This heat flux function tends to translate the stratified-wavy to annular transition boundary to lower vapor qualities with increasing heat flux. They also proposed an additional term to translate the boundary vertically upward by 50 kg/m^2 s to better match their observations. Their transition boundary for horizontal flow ($v = 0$) is:

$$G_{\text{Wavy,Kattan}} = \left[\frac{16\tilde{A}_{\text{V}}^3 gD\rho_{\text{L}}\rho_{\text{V}}}{\pi^2 x^2\sqrt{1-(2\tilde{h}_{\text{L}}-1)^2}}\times\left[1+\frac{\pi^2}{25\tilde{h}_{\text{L}}^2}(1-x)^{G_1}\left[\left(\frac{Fr}{We}\right)_{\text{L}}\right]^{G_2}\right]\right]^{1/2}+50. \tag{14}$$

As this transition boundary was not effective for ammonia, Zürcher et al. [8] proposed an empirical correction as follows:

$$G_{\text{Wavy,Zürcher et al.}} = G_{\text{Wavy,Kattan}} - 75\exp\left\{-\left[\frac{(x^2-0.97)^2}{x(1-x)}\right]\right\}. \tag{15}$$

Still, the heat flux correction defined with Eqs. (11) and (12) was too strong for a reasonable prediction of the onset of dryout region.

3.3. Equation of the A–I transition

Steiner [7] and Kattan et al. [1] proposed the intermittent to annular flow pattern transition to occur at a fixed value of the Martinelli parameter ($X_{tt} = 0.34$ for both phases turbulent and $X_{tt} = 0.51$ for laminar liquid and turbulent vapor flow) such that:

$$X_{tt} = \left(\frac{\mu_{\text{L}}}{\mu_{\text{V}}}\right)^{0.125}\left(\frac{1-x}{x}\right)^{0.875}\left(\frac{\rho_{\text{V}}}{\rho_{\text{L}}}\right)^{0.5} = 0.34. \tag{16}$$

This value is quite far from the one proposed by Taitel and Dukler [3] ($X_{tt} = 1.6$) but the experimental observations were much better predicted using Eq. (16).

3.4. Equation of the A–MF transition

The following equation has been proposed by Steiner [7] for the annular to mist flow pattern transition:

$$G_{\mathrm{MF,Steiner}} = \left[\frac{7680 \tilde{A}_{\mathrm{V}}^2 g D \rho_{\mathrm{L}} \rho_{\mathrm{V}}}{x^2 \pi^2 \xi_{\mathrm{Ph}}} \left(\frac{Fr}{We} \right)_{\mathrm{L}} \right]^{0.5}, \tag{17}$$

where ξ_{Ph} is the friction factor for rough pipes given by Prandtl and Nikuradse:

$$\xi_{\mathrm{Ph}} = \left[1.138 + 2 \log \left(\frac{\pi}{1.5 \tilde{A}_{\mathrm{L}}} \right) \right]^{-2}. \tag{18}$$

Kattan et al. [1] used the same equation but added a criterion to avoid the possibility of a mist flow reverting back again to annular flow with increasing vapor quality. Therefore, once the minimum value of the mass velocity is reached with Eq. (17), this minimum value is then applied at all higher vapor qualities. Thus, at the end of evaporation this transition curve is flat. It must be noted that this transition boundary has not been investigated experimentally in this work because of a limited pump capacity.

3.5. General comments about the Kattan et al. flow map

If the criteria proposed by Taitel and Dukler [3] are still recognized, their limitation for the prediction of the data collected in our laboratory has been shown in Kattan et al. [1]. It has been experimentally observed that the offset of Kattan et al. [1] (see Eq. (14)) is appropriate to the HFC-407C and HFC-134a refrigerants, but not for ammonia. The method of Steiner produced the inverse conclusion (good for ammonia and poor for HFC's). Also to be mentioned, the heat flux correction for the onset of dryout at high vapor quality seems to be too strong for ammonia where much more data have been obtained in the present investigation than in Kattan et al. [1]. Fig. 5 shows a comparison of the stratified-wavy to annular transition of Kattan et al. to that of Steiner for ammonia.

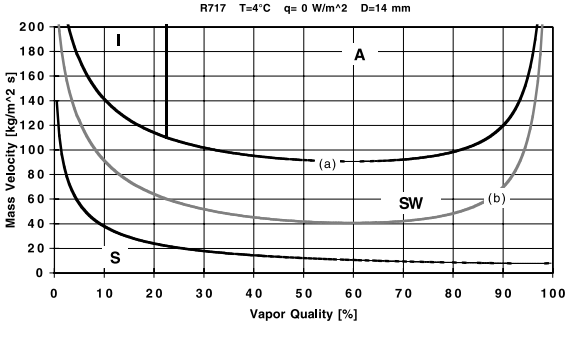

Fig. 5. Flow map without heat flux applied to ammonia with SW–A transition of Kattan (a) and Steiner (b).

4. New flow pattern map transition criteria

Several transition criteria use the void fraction to determine dimensionless velocities or cross-sectional surface areas. In the form proposed by Taitel and Dukler [3], Steiner [7] or Kattan [2], these parameters are based on the stratified configuration (liquid height prediction in a stratified configuration as in Fig. 1 in itself defines the void fraction).

Zuber and Findlay [9] explained with the notion of a *distribution parameter* that void fraction is dependent on flow pattern. This point has been experimentally observed through pressure level jumps when crossing given flow pattern transitions. The intermittent to annular transition had strong effects with pressure level jumps up to 0.5 bar while the stratified to stratified-wavy and the stratified-wavy to annular transitions had no noticeable effects.

This means that void fraction is not a continuous function during flow pattern transition, and that different void fraction models, based on flow pattern should be used. This is in agreement with the conclusions of Zuber and Findlay [9]. For example, it would be possible to define the stratified to stratified-wavy transition with the Taitel and Dukler [3] model (based on a stratified cross-section) and then to define the stratified-wavy to annular transition with an annular void fraction model as proposed for instance by Tandon et al. [10]. More specifically, it means that any flow pattern transition could be defined by two lines as the transitions might be analyzed from both flow directions, and thus gives rise to prediction of a transition zone that is typical of experimental observations. However, this approach would lead to a new level of complexity that is not presently justifiable.

As Zuber and Findlay [9] proposed that the void fraction can be different for different flow patterns, it means that the dimensionless parameters used by Taitel and Dukler [3] do not take into account the representative velocities or cross-sectional areas for other transitions, for example the stratified-wavy to annular one. Furthermore, the Zuber and Findlay drift flux model demonstrates clearly that void fraction is a function of mass velocity. Neither the model proposed by Taitel and Dukler [3], nor the one proposed by Steiner, are a function of mass velocity. Thus, it is important to define the most consistent void fraction model adapted to each flow pattern in predicting flow regimes transitions.

4.1. The new stratified to stratified-wavy transition

This transition is analysed from the stratified flow region. Thus, the void fraction model of Taitel and Dukler [3] is adopted. Since there is no particular advantage in the use of the non-dimensional variables proposed by Taitel and Dukler [3], Eq. (19) is similar to the original expression for horizontal flow, but expressed in terms of void fraction and dimensional perimeters:

$$X_{tt}^2\left[\frac{(S_L)^{1.2}}{(1-\alpha)^3}\right]-\left[\frac{(S_V+S_i)^{0.2}}{\alpha^2}\left(\frac{S_V+S_i}{\alpha}+\frac{S_i}{(1-\alpha)}\right)\right]=0. \tag{19}$$

This also means that the void fraction model of Taitel and Dukler can be used in the stratified flow regime and along the stratified to stratified-wavy boundary.

Thus, the stratified to stratified-wavy transition is similar to the one used by Kattan and developed by Steiner (see Eq. (7)). Nevertheless, it is more appropriate to represent Eq. (7) in terms of void fraction as:

$$G_{Strat}=\left[800\cdot\frac{\alpha^2(1-\alpha)}{x^2(1-x)}\cdot\rho_V g(\rho_L-\rho_V)\mu_L\cdot\cos v\right]^{1/3}, \tag{20}$$

where $\cos v = 1$ for horizontal flow. In this formulation, the effect of void fraction on the transition boundary is more explicit.

4.2. The new intermittent to annular transition

As the original transition proposed by Kattan [2] provided accurate results, the criterion based on the Martinelli parameter and the equation originally proposed by Steiner [6] (see Eq. (16)) is adopted here.

4.3. The new stratified-wavy to annular transition

This transition is analysed as being approached from the annular flow regime. As the interfacial interaction terms are important, this flow pattern should not be represented with the separated flow model. Annular flow is better represented by the drift flux model (which is a reduced formulation of the two-fluid model) as proposed by Ishii [11]. Consequently, the void fraction model proposed by Rouhani and Steiner will be used in the region of annular flow and along the stratified-wavy to annular boundary:

$$\alpha_{Rouhani}=\frac{x}{\rho_V}\left[(1+0.12(1-x))\left[\frac{x}{\rho_V}+\frac{1-x}{\rho_L}\right]+\frac{1.18(1-x)[g\sigma(\rho_L-\rho_V)]^{1/4}}{G\rho_L^{1/2}}\right]^{-1}. \tag{21}$$

Based on the model proposed by Steiner [7], which takes into account the surface tension and the gravity forces and assuming that the void fraction model of Rouhani/Steiner is a good representation of the effective void fraction, the new stratified-wavy to annular transition has been modified with the addition of a dissipation function along the length of a wave. The same procedure to account for the effect of heat flux developed by Kattan et al. [1] is used here but with a reduced influence compared to the original one. Very good agreement for both HFC-134a and ammonia has been found with the following expression:

$$G_{Wavy,New}=\left[\frac{gD\rho_L\rho_V\alpha^3\pi}{2x^2\sqrt{2(1-\cos\theta_{wet})}}\left(1+\frac{\pi^2}{25\tilde{h}_L^2}(1-x)^{G_1}\left(\frac{Fr}{We}\right)_L^{G_2}+\frac{\tilde{h}_L\lambda G^2x^2}{B_r\cdot\rho_V\alpha^{5/2}}\right)\right]^{1/2} \tag{22}$$

with $B_r = 3.0$ Pa. The first two terms in the bracket are equivalent to that in Eq. (14) written in terms of void fraction and wetting angle, while the last term represents the dissipation function. Assuming an annular core of the vapor and a smooth and motionless interface, the pressure drop is calculated along the liquid wave length, while the value of B_r is obtained in agreement with the flow pattern vizualisations of refrigerants HFC-134a and ammonia.

Fig. 6 shows the influence of the dissipation function on the stratified-wavy to annular flow pattern transition in adiabatic conditions with the use of the void fraction

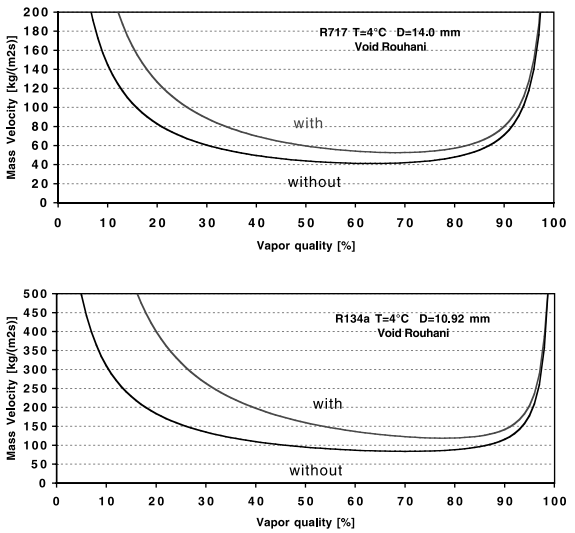

Fig. 6. Effect of the dissipation term of Eq. (22) on the stratified-wavy to annular transition in adiabatic conditions for ammonia (upper part) and HFC-134a (lower part).

expression of Rouhani. The inclusion of the dissipation term raises the transition threshold for both fluids. The friction factor λ is calculated with the following relation (turbulent flow and smooth pipe assumption):

$$\lambda = (1.8 \log Re_D - 1.64)^{-2}, \tag{23}$$

where Re_D is the liquid Reynolds number in annular configuration (given in Eq. (27)).

The heat flux functions G_1 and G_2 will only be used above a minimum non-dimensional value defined as:

$$\frac{\dot{q}}{\dot{q}_{\text{crit}}} \geqslant 0.0374 \tag{24}$$

i.e. above the heat flux required for the onset of nucleate boiling. For heat fluxes above this level, the two following relations will be used to move the onset of dryout (and hence the transition line) to lower vapor qualities:

$$G_1 = -24.12\left(\frac{\dot{q}}{\dot{q}_{\text{crit}}}\right), \tag{25}$$

$$G_2 = 4.825\left(\frac{\dot{q}}{\dot{q}_{\text{crit}}}\right) + 1. \tag{26}$$

Comparing these two Eqs. (11) and (12), the heat flux effect has been weakened here to reflect the trend observed in our new and larger database. If the heat flux is below this threshold, the two heat flux functions G_1 and G_2 are equal to zero, and, respectively, to one, which means, based on Eq. (22), that the Froude to Weber ratio is not affected by the heat flux. Note that the critical heat flux $\dot{q}_{\text{crit}}$ has already been defined with Eq. (13).

The onset of dryout at the end of evaporation follows the idea of Hsu [12], where it has been shown that a thin liquid layer tends to decay in the presence of a hot spot at the wall. This is due to the interfacial surface tension, which is locally affected by the temperature gradient. In the case of a turbulent liquid layer, a dry spot appears at the top of the tube when the heat flux is above that given in Eq. (24), which represents the onset of dryout (based on our experimental flow visualizations and heat transfer coefficients results). Below this heat flux, the database showed that the onset of dryout occurs for a constant value of Reynolds number of $Re_{DL} \approx 650$, which is thought to represent the turbulent/laminar transition of the liquid in two-phase flow. In this case, the temperature gradient in the liquid layer between the turbulent and the laminar regions of the film is sufficient to create enough interfacial stress to lead to the onset of dryout at low heat flux.

In annular flow the liquid layer thickness is rather small compared to the tube radius. In such conditions, a Reynolds number can be defined using the thickness of the liquid layer as the characteristic dimension. From the continuity equation and the definition of vapor quality and void fraction, the Reynolds number Re_{DL} is:

$$Re_{DL} = \frac{4\rho_L u_L \delta}{\mu_L} = \frac{4G\delta}{\mu_L}\frac{1-x}{1-\alpha} = \frac{G(1-x)D}{\mu_L}. \tag{27}$$

Thus, Eq. (22) is only applied to the case where the liquid flow is turbulent ($Re_{DL} > 650$). If the above equation leads to liquid Reynolds numbers lower than 650, then the boundary will follow the turbulent/laminar transition:

$$G_{\text{Wavy,New}} = \frac{650\mu_L}{(1-x)D}. \tag{28}$$

This last equation concerns only the onset of dryout part of the transition, and presents a smooth transition with Eq. (22). Fig. 7 shows the effect of heat flux on the stratified-wavy to annular transition boundary, which determines the onset of dryout at the end of evaporation.

With these modifications, accurate prediction of the flow pattern transition has been obtained for two dissimilar refrigerants (ammonia and HFC-134a) over a wide range of mass velocities, vapor qualities and heat fluxes based on an analysis of the flow.

4.4. The new annular to mist flow transition

Since this transition was not experimentally reached in the present tests, the original expression used by Kattan [2] is adopted here (see Eqs. (17) and (18)). The use of non-dimensional variables as defined through the stratified cross-section presents no particular advantage and thus, these two equations can be

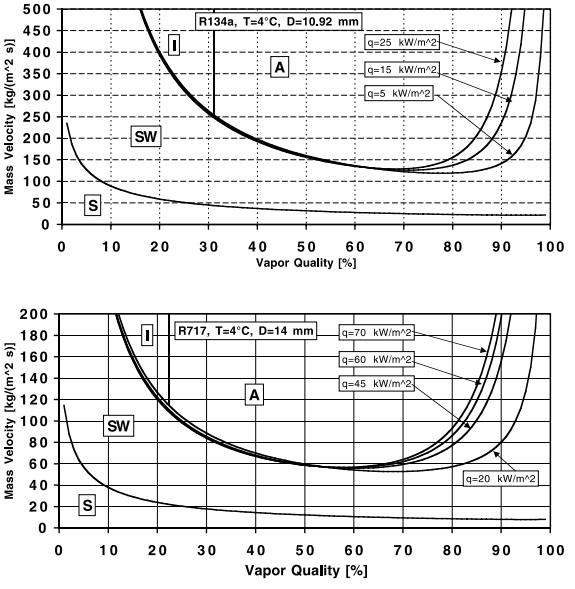

Fig. 7. Effect of heat flux on the stratified-wavy to annular transition boundary of the new flow map applied to the refrigerant HFC-134a and to ammonia.

directly expressed in terms of void fraction in one expression as:

$$G_{\mathrm{MF}} = \frac{\alpha}{x}\left[1.138 + 2\log\left(\frac{8}{3(1-\alpha)}\right)\right] \times \left[480gD\rho_{\mathrm{L}}\rho_{\mathrm{V}}\left(\frac{Fr}{We}\right)_{\mathrm{L}}\right]^{0.5}. \quad (29)$$

5. Implementation of the new flow map

The new flow pattern map transition boundaries can be calculated once the tube diameter, the vapor quality, the saturation temperature and the mean heat flux are defined and the other physical properties of the fluid are obtained at the operating temperature. The critical heat flux is also evaluated with the method of Kutateladze (see Eq. (13)).

The stratified to stratified-wavy boundary is first calculated with the void fraction model proposed by Taitel and Dukler [3] (see Eq. (19)). As this void fraction model is independent of mass velocity, only the void fraction equation has to be iterated for each different vapor quality.

Comparison of the desired mass velocity with the transitional value of the stratified to stratified boundary for a given vapor quality will show if the flow is stratified ($G < G_{\mathrm{Strat}}$) or not.

Another boundary easily obtainable is the intermittent to annular transition. This boundary is calculated with Eq. (16) with an explicit expression. With respect of the other boundaries, the flow will be intermittent for $x < x_{\mathrm{I/A}}$.

The mist flow boundary G_{MF} has to be found by iteration since the void fraction model of Rouhani depends on the mass velocity. For each vapor quality, an initial mass velocity is chosen ($G_{\mathrm{MF,init}} = 1000$ is a convenient value). With this value, the void fraction of Rouhani is calculated (Eq. (21)) and then the boundary (Eq. (29)). The new mass velocity is then used to recalculate the void fraction of Rouhani, and so on until convergence of the new mass velocity and the value at the boundary. The convergence criterion used in this work is $|\Delta G| < 1$ kg/(m^2 s) between these values. The general shape of the mist flow boundary is a continuous decrease until vapor quality reaches about $x \approx 70\%$. There, a minimum is reached at ($x_{\mathrm{MF,min}}, G_{\mathrm{MF,min}}$). Normally, Eq. (29) would predict a rapid rise in the transition mass velocity for $x > x_{\mathrm{MF,min}}$. Since there is no reason that a mist flow should revert to annular flow with increasing quality as noted by Kattan et al. [1], this boundary is constraint at its minimum when $x > x_{\mathrm{MF,min}}$.

The stratified-wavy to annular (or intermittent) transition is quite similar to the mist flow boundary identification procedure. An initial mass velocity is first set to $G_{\mathrm{Wavy,init}} \approx 1000$ kg/(m^2 s). Then the void fraction is calculated with Rouhani (Eq. (21)). The liquid Reynolds number applied to annular flow is determined with Eqs. (27) and (28) is used only when $Re_{\mathrm{L}} < 650$. For higher Reynolds values, the ratio of the mean heat flux to the critical heat flux calculated with the relation of Kutateladze (Eq. (13)) is determined. If the non-dimensional heat flux is large as defined with Eq. (24), then the functions G_1, G_2 are calculated with Eqs. (25) and (26). If the non-dimensional heat flux is smaller than the threshold value for onset of nucleate boiling, then $G_1 = 0$ and $G_2 = 1$. Next Eq. (22) is evaluated and the mass velocity obtained is used as the new initial value in the void fraction model, and so on until convergence of successive mass velocities.

The following criteria must also be applied to the transition equations where they intersect:

- The stratified-wavy to annular boundary needs not be defined in the mist flow region. Thus, at the end of evaporation when $G_{\mathrm{Wavy}} > G_{\mathrm{MF}}$, the value of the mist flow boundary G_{MF} is adopted as the limit to the stratified-wavy to annular boundary G_{Wavy}.
- The intermittent to annular transition $x_{\mathrm{I/A}}$ is defined from the stratified-wavy to annular flow pattern boundary G_{Wavy} up to the mist flow boundary G_{MF}.

Fig. 8 summarizes the set of equations and the procedure to be followed for the implementation of the flow pattern map.

6. Experimental results

For a detailed description of the test facility and measurement accuracies, refer to Kattan et al. [1] and to Zürcher et al. [8]. All three refrigerants were evaporated at a saturation temperature of 4°C. HFC-134a and HFC-407C were tested inside a tube of diameter 10.92 mm over a heat flux range of 2–5 kW/m^2 and three mass velocities of 100, 200 and 300 kg/(m^2 s), in which stratified-wavy, intermittent and annular flow regimes were observed. The sight glasses at the end of the test section had the same internal diameter.

For ammonia, the tests were conducted for an internal tube and sight glass diameter of 14.00 mm, a heat flux range of 5–70 kW/m^2 and 11 mass velocities of 10, 20, 30, 40, 45, 50, 55, 60, 80, 120 and 140 kg/(m^2 s), in which stratified, stratified-wavy, intermittent and annular flow patterns were observed. Additional tests, varying the mass velocity at constant vapor qualities ($x = 20\%, 50\%, 80\%$), were made in particular to better characterize the transition boundaries between flow patterns. The flow patterns were observed and videotaped through glass sections at both ends of the 3.01 m long test tube, but only those at the exit were placed in the database since the inlet sight glass is located just after a transfer line from the preheater to the evaporator test section.

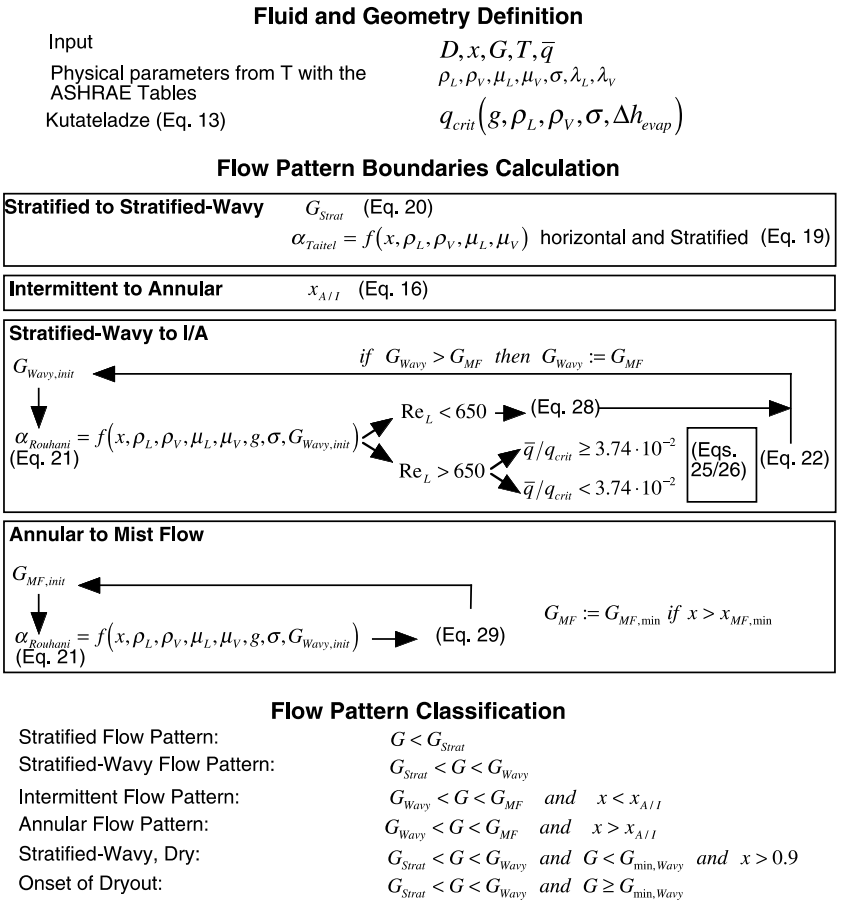

Fig. 8. Solution scheme for the new flow pattern map.

6.1. Ammonia and the new flow pattern map

Fig. 9 shows the flow patterns observed on a G vs. x map compared to the new transitional boundaries. The flow patterns observed experimentally and classified as S, SW, A and I are the clearly defined flow patterns. When the classification was not clear because of fluctuations from one regime to another near the transition zone, both patterns are noted, including preference to the dominant one. For example, a flow classified as X/Y is on the X to Y transition boundary, with an undetermined preference of both X and Y flow pattern. A flow classified as $X/(Y)$ is also on the same transition boundary, but this time the flow is dominantly X, with occasional occurrence of the Y flow pattern.

The transitions obtained on the map are based on a mean temperature value of 4°C, while a mean heat flux of 13.2 kW has been considered for the stratified-wavy to annular transition. Nevertheless, the difference between the mean experimental heat flux and the one defined for the map can be ignored as these are too low to displace the stratified-wavy to annular boundary (criterion defined in Eq. (24)).

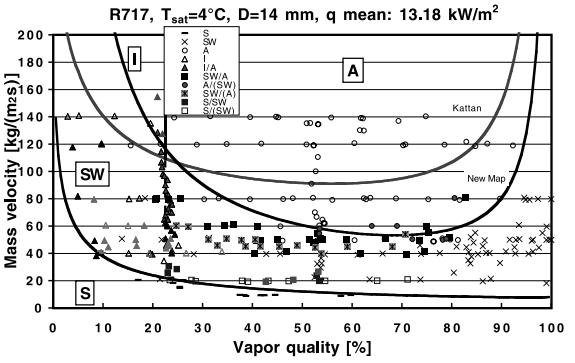

Fig. 9. Comparison of the Kattan et al. to the new method for the stratified-wavy to intermittent and annular flow transition boundary applied to flow pattern observations for ammonia.

The heat flux has been experimentally found to be of less importance than proposed by Kattan [1]. In ad-

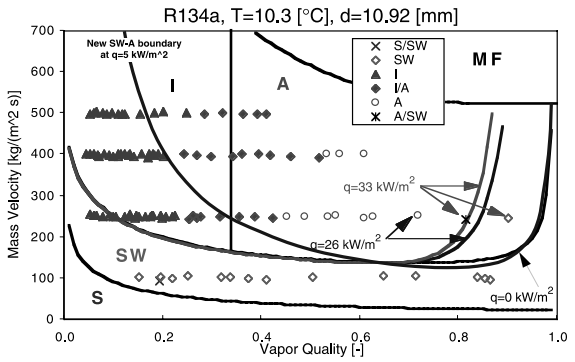

Fig. 10. Comparison of the Kattan et al. to the new method for the stratified-wavy to intermittent and annular flow transition boundary applied to flow pattern observations for HFC-134a.

dition, no effect on the onset of dryout of the stratified-wavy to annular transition has been detected when the heat flux was smaller than 45 kW/m^2.

The intermittent to annular transition agrees very well with the ammonia flow visualizations (as well as with the two refrigerants HFC-134a and HFC-407C), and further investigation regarding the existance of intermittent flow at lower mass velocities should be investigated, for example to extend its boundary down to the stratified to stratified-wavy boundary.

While not drawn on Figs. 9 and 10, the stratified to stratified-wavy flow transition proposed by Kattan [1] is similar to the present approach. This is logical as the void fraction defined by Steiner [6] is similar to the void fraction model proposed by Taitel and Dukler [3].

The stratified to stratified-wavy transition boundary is almost unchanged compared to the original one of Steiner [7] and is in agreement with the results of ammonia: the tests run at $G = 10$ kg/(m^2 s) were mostly stratified while the tests run at $G = 20$ kg/(m^2 s) where partially stratified and mostly stratified-wavy. As the boundary is nearly horizontal over a vapor quality change of $\approx 50\%$, its real location is very difficult to define. As no major change in experimental heat transfer coefficient is observed at these conditions, the accuracy in the definition of this boundary is of a lesser importance than for others.

The new flow pattern map based on the void fractions of Taitel and Dukler [3] and Rouhani [6] and including the effect of pressure drop along the wave length for the stratified-wavy to annular transition, showed very good agreement with the experimental flow pattern database for ammonia.

6.2. HFC-134a and the new flow pattern map

As the flow patterns observed with refrigerant HFC-407C were very similar to those obtained with refrigerant HFC-134a, only the second refrigerant is presented here for which more data are available.

Figs. 9 and 10 show a comparison of the map proposed by Kattan [2] and the new stratified-wavy boundary. The stratified-wavy to annular transition is obtained with Eqs. (14) and (22). The new boundary satisfies the observations of Kattan [2] at the lowest mass velocity ($G = 100$ kg/(m^2 s)) where the flow pattern is stratified-wavy, and it satisfies the higher mass velocities of $G = 200, 300$ kg/(m^2 s) where annular flow patterns occur. Their minimum values for this boundary is almost identical. Also, these predictions are in agreement with the observations of Mermond [13] who found the stratified-wavy to annular transition to be lower than $G = 150$ kg/(m^2 s).

It seems also here that the intermittent to annular transition could be extended until the stratified to stratified-wavy boundary as similarly proposed with the ammonia experimental results. In addition, referring to the limited observations reported by Mermond [13] for HFC-134a, we found very good agreement of the new flow pattern map with their flow pattern data.

7. Conclusions

A review of the flow maps proposed by Steiner [7] and Kattan et al. [1] has been presented and an improved flow pattern map in agreement with the natural refrigerant R717 has been proposed.

Taitel and Dukler, Steiner and Kattan et al. based their transitional phenomena on the separated flow model with the stratified geometry. With Kattan et al. [1], the flow pattern prediction was very accurate for the HFCs.

In this work, the stratified to stratified-wavy transition is similar to the model proposed by Taitel and Dukler [3] with the use of the sheltering coefficient defined by Steiner [7]. The void fraction model used is also the void fraction model defined by Taitel and Dukler [3] as the flow geometry of the stratified flow has been taken into account. The final expression of Taitel and Dukler [3], which is a function of non-dimensional cross-sectional areas, has been better expressed as a function of void fraction.

The intermittent to annular transition has been defined with the Martinelli parameter. Taitel and Dukler [3] defined the transitional value in a logical way which leads to a void fraction of $\tilde{h}_L \approx 0.5$, while Steiner argued experimental tests called for a smaller value of $\tilde{h}_L \approx 0.25$. Due to very good agreement with the ammonia and the HFC-134a database, the value of Steiner has been adopted in the new flow map.

As the annular to mist flow transition has not been reached in our experimental facility, no further modifications to the method of Kattan et al. [1] were proposed here.

The stratified-wavy to annular transition has been calculated with the Rouhani void fraction equation, which is based on the drift flux model, that is more appropriate to represent annular flow than the separated flow model. The criterion of Taitel and Dukler [3] is based on the growth of infinitesimal waves due to the Bernoulli effect and compensated by gravity, while Steiner [7] included also the surface tension forces. As the general assumption of Steiner was a non-dissipative flow of incompressible vapor, two additional influential effects have been investigated: the compressibility and the shear stress pressure drop of the vapor flow. It has been concluded that only the shear stress dissipation is sufficiently influential and it has been added to the general expression proposed by Steiner [7]. Due to this modification, the stratified-wavy to annular transition has been found to be appropriate for the HFCs class of refrigerants like HFC-134a and HFC-407C, as well as for the natural refrigerant ammonia.

Based on our experimental results, no influence of heat flux on the stratified to stratified-wavy and on the intermittent to annular transitions has been found, while only a reduced effect has been found on the stratified-wavy to annular transition. The onset of dryout phenomenon seems to be driven by a turbulent to laminar transition occurring at $Re_L \approx 650$ until a given heat flux is reached, above which the approach proposed by Kattan et al. [1] has been adopted.

Acknowledgements

This work has been carried out with the partial financial support of the Swiss Federal Office of Energy (OFEN).

References

[1] N. Kattan, J.R. Thome, D. Favrat, Flow boiling in horizontal tubes. Part 1: development of a diabatic two-phase flow pattern map, J. Heat Transfer 120 (1998) 140–147.

[2] N. Kattan, Contribution to the heat transfer analysis of substitute refrigerants in evaporator tubes with smooth or enhanced tube surfaces, Ph.D. Thesis No. 1498, Swiss Federal Institute of Technology in Lausanne, Switzerland, 1996.

[3] Y. Taitel, A.E. Dukler, A model for predicting flow regime transitions in horizontal and near horizontal gas–liquid flow, AIChE J. 22 (1) (1976) 47–55.

[4] K. Hashizume, Flow pattern and void fraction of refrigerant two-phase flow in a horizontal pipe, Bull. JSME 26 (219) (1983) 1597–1602.

[5] V.V. Klimenko, M. Fyodorov, Prediction of heat transfer for two-phase forced flow in channels of different orientation, in: Proceedings of the 9th International Heat Transfer Conference, vol. 5, 1990, pp. 65–70.

[6] D. Steiner, in: VDI-Wärmeatlas (VDI Heat Atlas) Verein (edited by Deutscher Ingenieure, VDI-Gesellschaft Verfahrenstechnik und Chemieingenieurwesen (GCV), Translator: J.W. Fullarton), Chapter Hbb. Düsseldorf, 1993.

[7] D. Steiner, Zweiphasenströmung in Apparatenelementen, Hochschulkurs Wärmeübertragung II. Forschungs-Gesellschaft Verfahrenstechnik e.V. Düsseldorf, 1983.

[8] O. Zürcher, J.R. Thome, D. Favrat, Evaporation of ammonia in a smooth horizontal tube: heat transfer measurements and predictions, J. Heat Transfer 121 (1999) 89–101.

[9] N. Zuber, J.A. Findlay, Average volumetric concentration in two-phase flow systems, J. Heat Transfer 87 (1965) 453–468.

[10] T.N. Tandon, H.K. Varma, C.P. Gupta, A void fraction model for annular two-phase flow, Int. J. Heat Mass Transfer 28 (1) (1985) 191–198.

[11] S. Kakaç, F. Mayinger, Two-Phase Flows and Heat Transfer, vol. 1, Hemisphere, Washington, DC, 1977.

[12] Y.Y. Hsu, F.F. Simon, J.F. Lad, Destruction of a thin liquid film flowing over a heating surface, Chem. Eng. Progr. Symp. Ser. 57 61 (1965) 139–152.

[13] Y. Mermond, Transferts de chaleur dans un mélange constitué de fluide frigorigène et d'huile, Thèse de l'Université Henri Poincarré, Nancy-I, 1999.